ISSN 0022-4766, Journal of Structural Chemistry, 2025, Vol. 66, No. 4, pp. 788-802. © Pleiades Publishing, Ltd., 2025.
Russian Text © The Author(s), 2025, published in Zhurnal Strukturnoi Khimii, 2025, Vol. 66, No. 4, 143688.

STRUCTURAL FEATURES OF COPPER(II) COMPLEXES BASED ON 3-(5-PHENYL-2*H*-TETRAZOL-2-YL)PYRIDINE AND 2,2′-BIPYRIDINE/1,10-PHENANTHROLINE*

E. A. Ermakova[1], K. S. Smirnova[1], L. S. Klyushova[2], I. S. Chernov[3], V. A. Ostrovskii[3], and E. V. Lider[1]**

Complex compounds $[CuL(phen)(H_2O)(NO_3)]NO_3$ (**1**), $[CuL(bipy)(NO_3)_2]\cdot 2EtOH$ (**2**), $[CuL_2(H_2O)_2(NO_3)_2]$ (**2a**), $[CuL(dmbipy)(NO_3)_2]\cdot 3EtOH$ (**3**), and $[CuL_2(NO_3)_2]$ (**3a**), where L is 3-(5-phenyl-2H-tetrazol-2-yl)pyridine, phen is 1,10-phenanthroline, bipy is 2,2′-bipyridine, and dmbipy is 4,4′-dimethyl-2,2′-bipyridine, are obtained and structurally characterized. It is shown that L behaves as the monodentate ligand being coordinated by the nitrogen atom of the pyridine ring. The coordination polyhedron made of copper atoms is a square pyramid in complexes **1** and **3,** a distorted octahedron and a distorted square in complexes **2a** and **3a** respectively. Complex **1** is characterized by the elemental analysis, powder X-ray diffraction, and IR spectroscopy. Furthermore, its cytotoxic properties are studied on human larynx carcinoma (Hep2), breast adenocarcinoma (MCF7), and non-tumor human fibroblast (MRC5) cell lines. Complex **1** is shown to exhibit the pronounced cytotoxic action (LC_{50}(Hep2) = 4.1±0.4 μM and LC_{50}(MCF7) = 4.9±0.1 μM), however, does not exhibit selectivity against tumor cell lines (LC_{50}(MRC5) = = 3.06 ±0.02 μM).

DOI: 10.1134/S0022476625040146

Keywords: copper(II) complexes, tetrazole, pyridine, crystal structure, cytotoxicity, selectivity index.

INTRODUCTION

Tetrazoles attract the attention of more and more researchers owing to their numerous properties allowing their application in producing nanoparticles [1-3], catalysts [4-6], and so on. Some tetrazoles have traditionally been considered and applied as components of high-energy systems and materials because large amounts of energy stored in the ring and molecular nitrogen are released during their decomposition [7, 8]. However, their application is most promising in medicinal chemistry because they possess antimicrobial [9-13], antiviral [13-17], anti-inflammatory [13, 18-21], antifungal [13, 22-25],

[1]Nikolaev Institute of Inorganic Chemistry, Siberian Branch, Russian Academy of Sciences, Novosibirsk, Russia; **lisalider@gmail.com. [2]Institute of Molecular Biology and Biophysics, Federal Research Center of Fundamental and Translational Medicine, Novosibirsk, Russia. [3]St. Petersburg State Institute of Technology (Technical University), St. Petersburg, Russia. Original article submitted November 25, 2024; revised December 12, 2024; accepted December 24, 2024.

* Supplementary materials for this article are available at doi 10.1134/S0022476625040146 and are accessible for authorized users.

and other activities. Moreover, the tetrazolyl fragment is the key one in many potential drugs for treating diabetes mellitus [26]. The tetrazole moiety is more and more often included in the composition of potentially antitumor drugs during their elaboration [13, 27-29]. For instance, A. Kamal's research group has developed benzothiazole hybrids with the tetrazole ring which inhibit tubulin, thus exhibiting the antiproliferative activity [30]. Hence, the synthesis of compounds with the tetrazole moiety is promising: they can be expected to exhibit the pronounced biological activity.

Our research group has previously obtained and characterized mixed-ligand copper(II) complexes based on 1,10-phenanthroline/2,2′-bipyridine and various tetrazole derivatives: 5-methyltetrazole [31], 5-benzyltetrazole [32], 5-phenyltetrazole [33], 5-(4-chlorophenyl)-1*H*-tetrazole [34], 1*H*-tetrazolyl-5-acetic acid [35]. Their cytotoxic activity was studied in vitro against diverse tumor cell lines. In the context of our interest in preparing the most cytotoxic and selective tetrazole-based copper(II) complexes, in this work, we describe the synthesis of five new coordination compounds: $[Cu(Ch)(phen)(H_2O)NO_3]NO_3$ (**1**), $[CuL(bipy)(NO_3)_2]\cdot 2EtOH$ (**2**), $[CuL_2(H_2O)_2(NO_3)_2]$ (**2a**), $[CuL(dmbipy)(NO_3)_2]\cdot 3EtOH$ (**3**), and $[CuL_2(NO_3)_2]$ (**3a**), where L is 3-(5-phenyl-2H-tetrazol-2-yl)pyridine, phen is 1,10-phenanthroline, bipy is 2,2′-bipyridine, dmbipy is 4,4′-dimethyl-2,2′-bipyridine. The structures of all complexes were determined by the single crystal X-ray diffraction (XRD) analysis, and complex **1** is characterized by standard physicochemical techniques (elemental analysis, powder XRD, IR spectroscopy) and its cytotoxic activity is studied on Hep2, MCF7, and MRC5 cell lines.

EXPERIMENTAL

To synthesize the complex we used commercially available copper(II) nitrate trihydrate (analytical grade) and organic ligands: 3-(5-phenyl-2*H*-tetrazol-2-yl)pyridine (L) and 1,10-phenanthroline (phen, 98%), 2,2′-bipyridine (bipy, 99%), and 4,4′-dimethyl-2,2′-bipyridine (dmbipy, 98%). 3-(5-Phenyl-2H-tetrazol-2yl)pyridine (Fig. 1) was synthesized by the procedure reported in [36] and structurally characterized by single crystal XRD.

Synthesis of $[CuL(phen)(H_2O)NO_3]NO_3$ (1). To a solution of 1,10-phenanthroline (0.10 mmol, 0.018 g in 2.0 mL of ethanol) copper(II) nitrate (0.10 mmol, 0.024 g) was poured, and a solution of L (0.10 mmol, 0.023 g in 3.0 mL of ethanol) was added to it in several minutes with constant magnetic stirring. The reaction mixture obtained was left for slow crystallization at room temperature. In a week, $[Cu(Ch)(phen)(H_2O)NO_3]NO_3$ (**1**) single crystals suitable for the XRD analysis were obtained, which were filtered off, washed with ethanol, and dried in the air.

Calculated for $C_{24}H_{19}CuN_9O_7$ (%): C 47.3, H 3.1, N 20.7. Found (%): C 47.4, H 2.9, N 20.7. Yield: 0.030 g (48%). IR absorption bands (ν, cm^{-1}): 3285 ν(OH); 3091, 3055, 3034, 2922, 2852 ν(CH); 1635, 1612, 1583, 1558, 1521, 1489 R_{ring};1397, 1384, 846 ν(NO_3).

Synthesis of $[CuL(bipy)(H_2O)NO_3]NO_3$ (2). To a solution of 2,2′-bipyridine (0.10 mmol, 0.016 g in 2.0 mL of ethanol) copper(II) nitrate (0.10 mmol, 0.024 g) was poured, and a solution of L (0.10 mmol, 0.023 g in 3.0 mL of ethanol) was added to it in several minutes with constant magnetic stirring. The reaction mixture obtained was left for slow crystallization at room temperature. In a week, two types of single crystals suitable for the single crystal XRD analysis were obtained: $[CuL(bipy)(NO_3)_2]\cdot 2EtOH$ (**2**) and $[CuL_2(H_2O)_2(NO_3)_2]$ (**2a**).

Synthesis of $[CuL(dmbipy)(NO_3)_2]\cdot 3EtOH$ (3). To a solution of 4,4′-dimethyl-2,2′-bipyridine (0.10 mmol, 0.018 g in 2.0 mL of ethanol) copper(II) nitrate (0.10 mmol, 0.024 g) was poured, and a solution of L (0.125 mmol, 0.029 g in 3.0 mL of ethanol) was added to it in several minutes with constant magnetic stirring. The reaction mixture was evaporated upon heating to 80 °C on a magnetic stirrer to a 1/3 volume loss. The solution obtained was left for slow crystallization at room

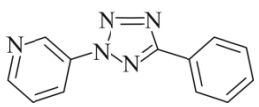

Fig. 1. Structure of 3-(5-phenyl-2*H*-tetrazol-2-yl)pyridine (L).

temperature. In a week, two types of single crystals suitable for the single crystal XRD analysis were obtained: $[CuL_2(NO_3)_2]$ (**3a**) and $[CuL(dmbipy)(NO_3)_2]\cdot 3EtOH$ (**3**).

The elemental analysis was performed on a Vario MICRO cube CHN-analyzer in the Analytical Laboratory of the Nikolaev Institute of Inorganic Chemistry, Siberian Branch, Russian Academy of Sciences by the standard procedure. The IR spectra were recorded on a Scimitar FTS 2000 Fourier spectrometer in the range of 4000-400 cm^{-1} (suspensions in fluorinated oil or pellets in KBr). The powder XRD analysis of the complexes was carried out on a Bruker D8 Advance diffractometer (CuK_α radiation, Ni-filter, 2θ measurement range from 5° to 40°, 2θ step 0.03°, point acquisition time 1 s).

Absorption spectra of complex **1** in an aqueous solution and the phosphate-salt buffer (0.01 M phosphate buffer with pH 7.3-7.5, 0.137 M NaCl, 0.0027 M KCl) were recorded on a SF-102 spectrophotometer (cuvette length 1 cm) at room temperature with time (t = 0 h, 24 h, 48 h). The complex was pre-dissolved in dimethylsulfoxide, and then diluted with water or the buffer solution to a concentration of 20 μM.

The single crystal XRD analysis of the ligand and copper(II) coordination compounds was performed on a Bruker D8 Venture diftractometer (graphite-monochromatic MoK_α radiation, λ = 0.71073 Å) by the standard procedure. The measurements were carried out by φ- and ω-scanning. Absorption corrections were applied using the SADABS program [37]. The structures were solved and refined using SHELXTL program packages [38, 39] and the Olex2 program [40]. Atomic displacement parameters of non-hydrogen atoms were refined anisotropically. Positions of hydrogen atoms were calculated in accordance with their geometric positions and refined in the riding model. The outer spheres of complexes **2** and **3** contain disordered ethanol molecules. To remove the electron density corresponding to two (**2**) or three (**3**) ethanol molecules in the system, the Solvent Mask function was applied in the Olex2 program. In coordination compound **3**, one nitrate group coordinated to Cu2 is disordered with ratio ≈0.8:0.2. Crystallographic data for the ligand and copper(II) complexes and information about the refined structures are summarized in Table 1; Cu–O and Cu–N bond lengths in the complexes, distances in hydrogen bonds and π–π interactions are listed in Table 2. The single crystal XRD data have been deposited with the Cambridge Crystallographic Data Center (CCDC 2404299-2404304); they can be obtained free of charge at http://www.ccdc.cam.ac.uk/data_request/cif.

TABLE 1. Crystallographic Data and Structure Refinement Results for the Ligand and Copper(II) Complexes

Parameter	**L**	**1**	**2**	**2a**	**3**	**3a**
1	2	3	4	5	6	7
Chemical formula	$C_{12}H_9N_5$	$C_{24}H_{19}CuN_9O_7$	$C_{26}H_{29}CuN_9O_8$	$C_{24}H_{22}CuN_{12}O_8$	$C_{30}H_{39}CuN_9O_9$	$C_{24}H_{18}CuN_{12}O_6$
M, g/mol	223.24	609.02	659.11	670.07	733.23	634.04
Crystal system	Monoclinic	Monoclinic	Triclinic	Triclinic	Triclinic	Monoclinic
Space group	$C2/c$	$P2_1/c$	$P\bar{1}$	$P\bar{1}$	$P\bar{1}$	$P2_1/n$
Temperature, K	150.0	150.0	293.0	150.0	150.0	150.0
a, b, c, Å	25.8884(9), 4.60500(10), 20.9945(7)	14.7529(4), 22.9345(7), 7.2368(2)	7.0415(14), 10.476(2), 19.639(4)	6.81880(10), 7.27870(10), 14.9240(3)	7.4657(2), 20.7566(5), 22.2562(6)	6.9416(2), 13.4716(4), 13.6923(4)
α, β, γ, deg	90, 123.1320(10), 90	90, 94.6160(10), 90	87.31(3), 83.64(3), 85.21(3)	89.0180(10), 87.9600(10), 67.0010(10)	63.0370(10), 80.7010(10), 83.1730(10)	90, 96.3240(10), 90
Volume, $Å^3$	2095.95(11)	2440.63(12)	1433.8(5)	681.39(2)	3029.51(14)	1272.64(6)
Z	8	4	2	1	4	2
ρ_{cal}, g/cm^3	1.415	1.657	1.313	1.633	1.305	1.655
μ, mm^{-1}	0.092	0.962	0.811	0.875	0.771	0.927
Crystal dimensions, mm	0.3×0.04×0.025	0.07×0.06×0.03	0.12×0.09×0.03	0.15×0.1×0.04	0.11×0.04×0.03	0.15×0.11×0.05
2θ scanning range, deg	3.76-54.22	3.29-52.90	4.18-54.39	5.46-66.43	3.73-56.67	5.99-63.03

TABLE 1. (Cont.)

1	2	3	4	5	6	7
h, k, l index range	$-32 \le h \le 32$, $-5 \le k \le 5$, $-26 \le l \le 26$	$-17 \le h \le 18$, $-28 \le k \le 28$, $-9 \le l \le 9$	$-8 \le h \le 9$, $-13 \le k \le 13$, $-25 \le l \le 25$	$-10 \le h \le 10$, $-11 \le k \le 11$, $-22 \le l \le 22$	$-9 \le h \le 8$, $-27 \le k \le 26$, $-29 \le l \le 21$	$-10 \le h \le 10$, $-18 \le k \le 19$, $-20 \le l \le 12$
Number of reflections measured / independent	14710 / 2309	26849 / 5002	11867 / 6271	15002 / 5197	26814 / 14846	8533 / 4176
R_{int}, R_σ	0.0617, 0.0432	0.0555, 0.0416	0.0753, 0.2706	0.0449, 0.0523	0.0443, 0.0917	0.0263, 0.0441
Number of restraints / parameters	0 / 154	0 / 371	0 / 343	1 / 208	4 / 754	0 / 196
Goodness on F^2	1.026	1.029	0.945	1.044	0.999	1.053
R-factors (for $I > 2\sigma(I)$)	$R_1 = 0.0434$, $wR_2 = 0.1038$	$R_1 = 0.0356$, $wR_2 = 0.0799$	$R_1 = 0.0566$, $wR_2 = 0.1172$	$R_1 = 0.0428$, $wR_2 = 0.0894$	$R_1 = 0.0614$, $wR_2 = 0.1451$	$R_1 = 0.0528$, $wR_2 = 0.1471$
R-factors (for all reflections)	$R_1 = 0.0670$, $wR_2 = 0.1165$	$R_1 = 0.0494$, $wR_2 = 0.0865$	$R_1 = 0.1059$, $wR_2 = 0.1294$	$R_1 = 0.0528$, $wR_2 = 0.0958$	$R_1 = 0.1045$, $wR_2 = 0.1713$	$R_1 = 0.0698$, $wR_2 = 0.1611$
Residual electron density (max / min), e/Å^3	0.17 / –0.18	0.31 / –0.40	0.76 / –0.50	0.49 / –0.43	0.41 / –0.47	1.00 / –0.91
CCDC	2404299	2404302	2404304	2404300	2404301	2404303

TABLE 2. Cu–O and Cu–N Bond Lengths in the Complexes, Distances in Hydrogen Bonds and π–π Interactions (Å)

Bond	**1**	**2**	**2a**	**3**	**3a**
Cu–N(L)	1.9915(19)	2.045(3)	1.9991(12), 1.9992(12)	2.011(3), 2.023(4)	2.010(2)
Cu–N(L^{N-N})	1.9980(19)	1.997(3),	–	2.025(3), 1.981(3)	
	2.034(2)	1.974(3)		2.001(3), 2.002(3)	
Cu–O(H_2O)	2.2519(16)	–	1.9768(11)	–	–
Cu–O(NO_3^-)	2.0016(17)	1.968(3)	2.4436(11)	2.379(3), 2.040(3)	1.9907(18)
		2.265(3)		2.196(5), 1.985(3)	
H–O···O	2.740	–	2.670, 2.736	–	–
	2.955				
Cg···*Cg*	3.657	3.650	3.677	3.555	–
	3.791				

Note: L^{N-N} is 1,10-phenanthroline, 2,2′-bipyridine, or 4,4′-dimethyl-2,2′-bipyridine.

Cytotoxic activity. In this work, we used human cell lines: Hep2 (larynx carcinoma), MCF-7 (breast adenocarcinoma), and MRC-5 (non-tumor lung fibroblasts) acquired from the State Research Center of Virology and Biotechnology VECTOR. They were cultured in the DMEM medium in the CO_2-incubator (37 °C, 5% CO_2, humid atmosphere). For the experiments the cells were cultured at a density of $5 \cdot 10^4$ cells per well in 96-well plates for 24 h under the standard conditions. Then the cells were added with the compounds in different concentrations obtained by serial dilution with cell culture medium (1-50 μM) and incubated for 48 h under the standard conditions. Fluorescent dyes (Hoechst 33342 (Sigma-Aldrich) and propidium iodide (Invitrogen)) were added for 30 min at 37 °C to estimate the cell viability. For the automatic visualization (four fields per well) we employed the IN Cell Analyzer 2200 (GE Healthcare, Great Britain) instrument. Finally, images were obtained in which the number of live, dead, and apoptotic cells were calculated using the In Cell Investigator software. The results are presented as average percentage of live, dead, and apoptotic cells (±standard deviation).

RESULTS AND DISCUSSION

Mixed-ligand complex **1** was obtained as single crystals from the reaction mixture by the following procedure: solid copper(II) nitrate was poured to the ethanol solution of 1,10-phenanthroline followed by the addition of 3-(5-phenyl-2*H*-tetrazol-2-yl)pyridine dissolved in ethanol with molar ratio Cu^{2+}:L:phen = 1:1:1.

The use of the same procedure for complex **2** resulted in the formation of two types of single crystals: $[CuL(bipy)(NO_3)_2]\cdot 2EtOH$ (**2**) and $[CuL_2(H_2O)_2(NO_3)_2]$ (**2a**). We failed to separate them. When molar ratio Cu^{2+}:L:phen was changed from 1:1:1 to 1:0.8:1, similar two types of single crystals were obtained. Variation of solvents resulted in the formation of precipitates whose compositions were not determined.

The reproduction of the synthesis procedure of complex **1** for the complex with 4,4′-dimethyl-2,2′-bipyridine (**3**) led to the formation of copper(II) nitrate single crystals, while a change in the Cu^{2+}:L:phen molar ratio from 1:1:1 to 1:1.25:1 yielded two types of single crystals: $[CuL(dmbipy)(NO_3)_2]\cdot 3EtOH$ (**3**) and a small amount of $[CuL_2(NO_3)_2]$ (**3a**).

Thus, we managed to isolate only pure mixed-ligand complex **1** and characterize it, and the other compounds were isolated as single crystals and described only be single crystal XRD. The $[CuL(phen)(H_2O)NO_3]NO_3$ compound is well soluble in dimethylsulfoxide, ethanol and poorly soluble in acetonitrile, water, and the phosphate-salt buffer. The experimental XRD pattern obtained of complex **1** coincides with the theoretical one calculated from the single crystal XRD data (Fig. 2), which confirms the phase purity of the compound. The elemental analysis data are consistent with the proposed formula for **1**. Moreover, the mentioned complex is characterized by IR spectroscopy, and stretching vibrations of CH groups and the aromatic ring in the ranges of 3091-2852 cm^{-1} and 1635-1489 cm^{-1}, respectively, are present in the spectrum. The stretching vibrations of the nitrate group are observed approximately at 1397-1384 cm^{-1} and 846 cm^{-1}. The spectrum also contains stretching vibrations near ~3285 cm^{-1} of the coordinated water molecule.

Crystal structures. The ligand structure was previously reported and described [36], however, in this work, single crystals were obtained with another space group (*C*2/*c*) and unit cell parameters. The π–π interaction is observed between two neighboring ligand molecules (Fig. 3): the distance between the tetrazole ring and the phenyl moiety is 3.675 Å (against 3.662 Å in [36]), and it is 3.631 Å (3.622 Å in [36]) between pyridine and tetrazole. The molecular packing of two modifications is depicted in Fig. 3*b*.

The 1,10-phenanthroline-based complex obtained is mononuclear and cationic $[Cu(phen)L(H_2O)(NO_3)]NO_3$ (**1**), with the nitrate group acting as a counterion (Fig. 4). The environment of the central metal atom contains two nitrogen atoms of the chelate-coordinated phen molecule, the nitrogen atom of the L pyridine ring, to oxygen atoms of the nitrate group, and the oxygen atom of the water molecule. The coordination polyhedron type can be determined using the SHAPE program: for compound **1** the minimum *S* parameter is observed for the polyhedron of the vacant octahedron type - 0.85. The second method to determine the coordination polyhedron type is the calculation of the τ_5-parameter where the largest angles of the

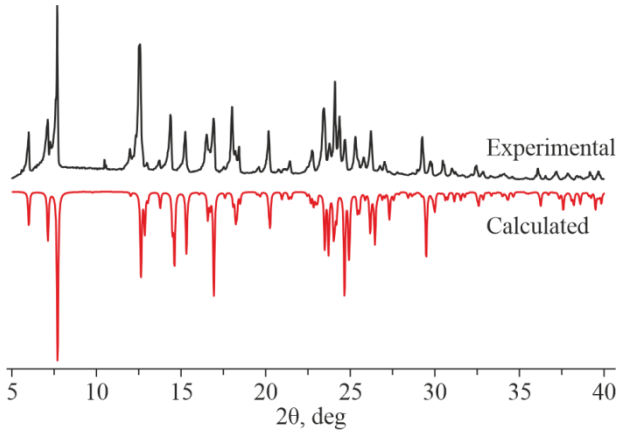

Fig. 2. XRD pattern of complex **1**.

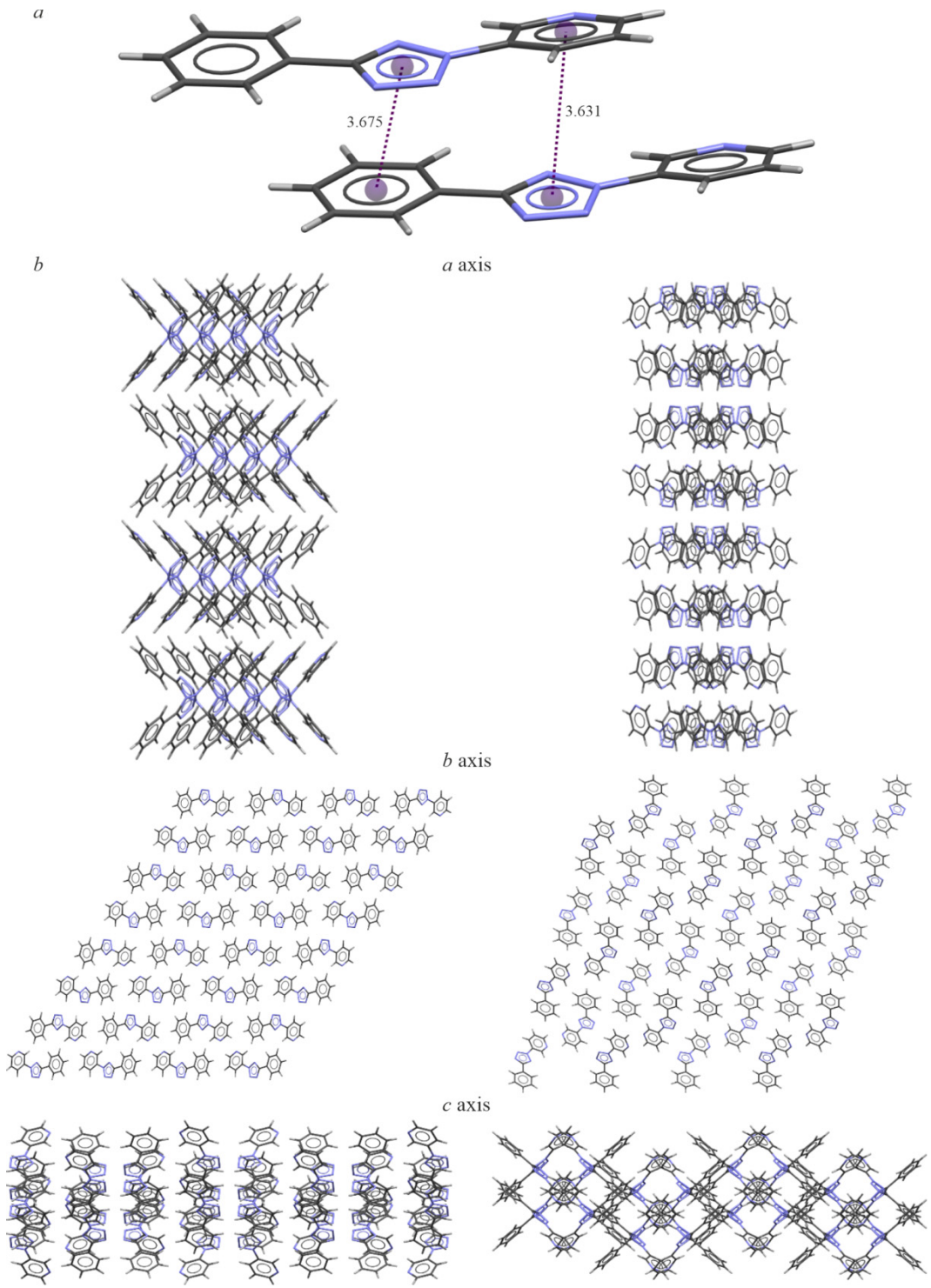

Fig. 3. Intermolecular π–π interaction between the neighboring ligand molecules (*a*) and molecular packings of its two modifications (*b*): *left* - this work, *right* - [36].

coordination core are used [41]. For complex **1** the τ_5-parameter is 0.063, which indicates the square pyramid. The distance between the copper(II) ion and the second oxygen atom of the nitrate group is 2.754 Å, which results in the 5 + 1 environment.

Oxygen atoms of coordinated and uncoordinated nitrate groups participate in the formation of hydrogen bonds with the water molecule (Fig. 5*a*). Moreover, there is the π–π interaction with a distance of 3.791 Å between phen molecules of

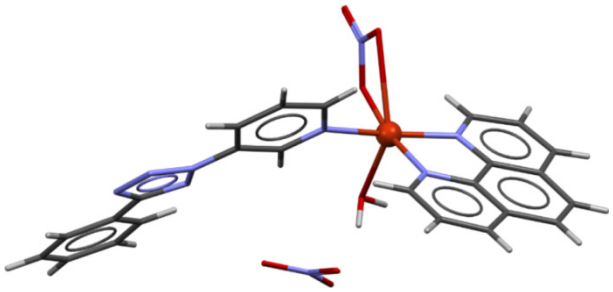

Fig. 4. Structure of $[Cu(phen)L(H_2O)(NO_3)]NO_3$ complex (**1**).

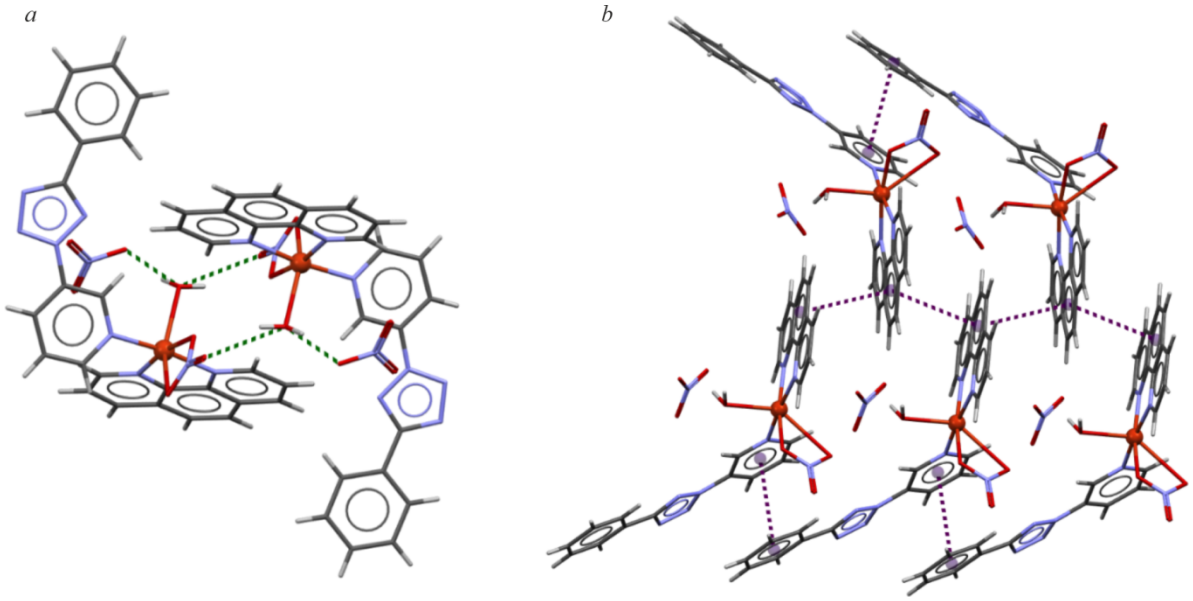

Fig. 5. Hydrogen bonds (*a*) and the π–π interaction (*b*) in the structure of complex **1**.

the neighboring complexes along with the π-stacking between pyridine of one molecule and the phenyl group of the adjacent ligand with a distance of 3.657 Å (Fig. 5*b*).

The coordination compound based on 2,2′-bipyridine $[Cu(bipy)L(NO_3)_2]\cdot 2EtOH$ (**2**) is mononuclear, however, unlike complex **1**, both nitrate groups are coordinated to the copper(II) ion. Apart from oxygen atoms, the coordination environment contains two bipy nitrogen atoms and the nitrogen atom of the pyridine ring of the L ligand (Fig. 6). We failed to unambiguously determine the coordination polyhedron type because the minimum *S* parameter is observed for three types: square pyramid (2.51), trigonal bipyramid (3.30), and vacant octahedron (3.28). Here the τ_5 parameter is 0.41, which also testifies the ambiguity of the coordination polyhedron.

As in the case of complex **1**, the distance between the copper(II) ion and the second oxygen atom of the nitrate group is 2.720 Å. Hence, the coordination environment can be represented as 5 + 1. The π-stacking with a distance of 3.650 Å is observed between the tetrazole and phenyl moieties of the neighboring ligand molecules (Fig. 7).

The general formula of complex **3** based on 4,4′-dimethyl-2,2′-bipyridine is similar to that of complex **2** - $[Cu(dmbipy)L(NO_3)_2]\cdot 3EtOH$. However, the system contains two crystallographically non-equivalent copper(II) ions (Fig. 8). For Cu1 the minimum *S* parameter is observed for three types of polyhedra: square pyramid (3.02), trigonal bipyramid (3.73), and vacant octahedron (3.74), and τ_5-parameter = 0.40. The Cu1 environment has two elongated Cu–O bonds (2.617 Å and 2.665 Å), which indicates the 5 + 2 coordination environment. For the Cu2 ion the coordination polyhedron corresponds to the square pyramid according to the calculated τ_5 parameter - 0.18, and the SHAPE analysis indicates the square pyramid

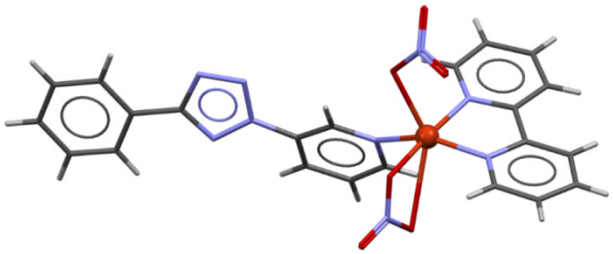

Fig. 6. Structure of [Cu(bipy)L(NO_3)$_2$]·2EtOH complex (**2**). Solvent molecules are omitted.

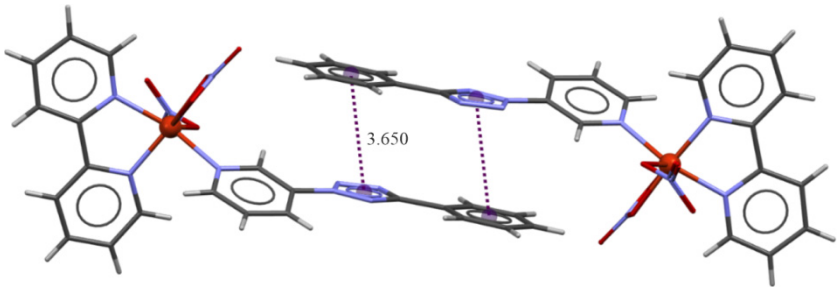

Fig. 7. Intermolecular π–π interactions in the structure of complex **2**.

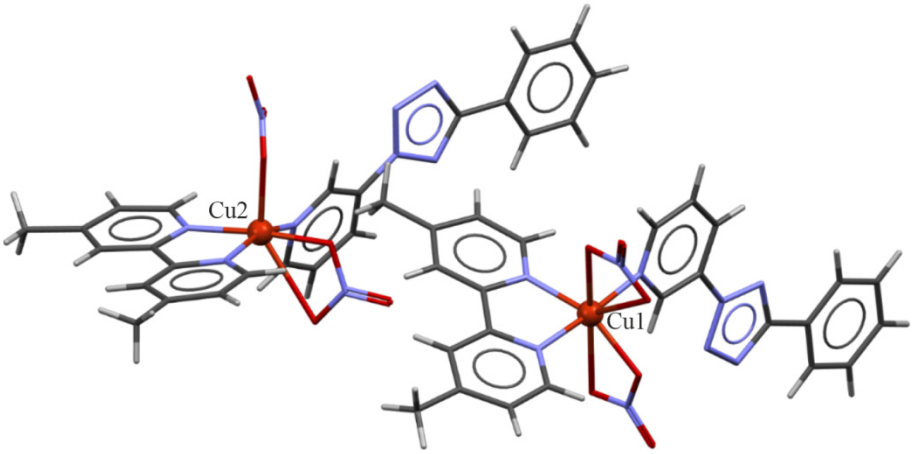

Fig. 8. Two crystallographically non-equivalent copper(II) ions in the structure of [Cu(dmbipy)L(NO_3)$_2$]·3EtOH complex (**3**). Solvent molecules are omitted.

(1.54) or the vacant octahedron (1.56). However, one elongated Cu–O bond (2.719 Å) is observed for Cu2, which confirms the 5 + 1 environment.

The intermolecular π–π interaction with a distance of 3.555 Å is noted between the phenyl and pyridine moieties of the neighboring ligands only for the complexes with Cu1 (Fig. 9).

During crystallization of complexes **2** and **3** single crystals different from the main phase were discovered: for compound **2** - complex [Cu(H_2O)$_2$L$_2$(NO_3)$_2$] (**2a**) and for complex **3** - [CuL$_2$(NO_3)$_2$] (**3a**). The organic ligand is monodentate coordinated by the nitrogen atom of the pyridine ring, as in the previously described compounds. The coordination polyhedron of complex **2a**, consisting of two ligand nitrogen atoms, two oxygen atoms of the nitrate groups, and two oxygen atoms of two water molecules, belongs to the octahedron with parameter $S(Oh) = 1.60$ (Fig. 10*a*). As in complex **1**, the presence of water molecules in the system leads to the formation of intermolecular hydrogen bonds between oxygen atoms of the nitrate group and the water molecule (Fig. 11*a*). Here the π–π interaction is similar to the π-stacking in complex **2** with a distance of 3.677 Å between the tetrazole and phenyl moieties (Fig. 11*b*). Water is absent in the composition of compound

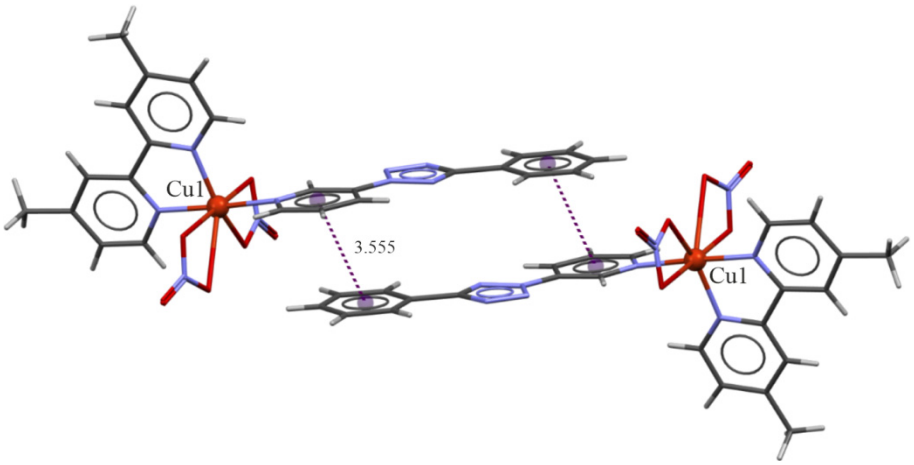

Fig. 9. Intermolecular π–π interactions in the structure of complex **3**.

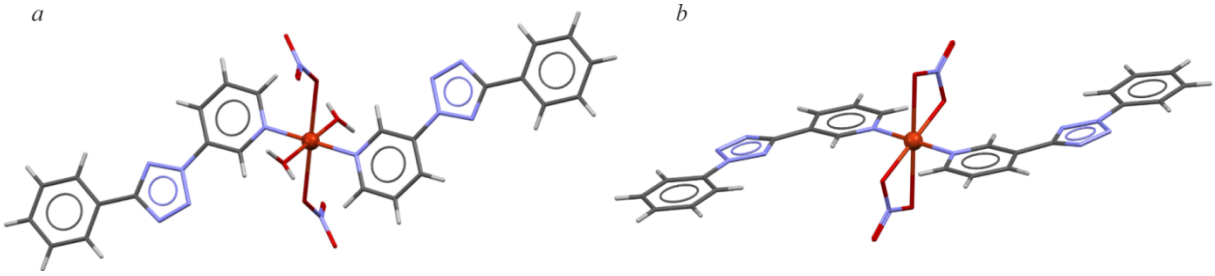

Fig. 10. Structures of $[Cu(H_2O)_2L_2(NO_3)_2]$ (*a*) and $[CuL_2(NO_3)_2]$ (*b*) complexes.

3a (Fig. 10*b*); the coordination polyhedron consisting of oxygen atoms of the nitrate group and nitrogen atoms of the ligand pyridine ring is a square with the zero τ_4 parameter [42], which is also supported by the SHAPE analysis with parameter *S*(*D*4*h*) = 0.005. The distance of 2.553 Å is observed between the second oxygen atom of the nitrate group and the copper(II) ion, which indicates coordination environment 4 + 2.

According to the CCDC data, for most copper(II) nitrate complexes the Cu–O(NO_2) bond length is within 1.97-2.03 Å, and there is a number of examples where its value reaches 2.8 Å (Fig. 11*c*).

Since for the further study of the cytotoxic activity it is needed to use solutions of the complexes, then it is important to take into account the stability of forms obtained in the solution. To this end, by optical spectroscopy we analyzed the aqueous and phosphate-salt solutions of complex **1** with different storage times. The concentrated solution of the complex in dimethylsulfoxide (*C* = 1 μM) was diluted with water or the phosphate-salt buffer up to 20 μM, and then the absorption spectra were measured with time (*t* = 0 h, 24 h, 48 h, Fig. 12).

The UV range of the spectra of complex **1** in the aqueous and phosphate-salt solutions demonstrate absorption bands at 234 nm and 272 nm, which correspond to the π–π* electron transition (Table 3). Substantial changes are observed in the spectra of complex **1** in both solutions: the absorption intensity decreases by on average 20% in 48 h. Its maximum decrease of 22.5% was observed in the UV range of the spectrum of the aqueous solution. Consequently, it can be supposed that the form appeared in the solution is unstable.

Cytotoxic activity. The effect of ligands, copper(II) nitrate, and complex **1** on the cell viability was studied on the cell lines of human larynx carcinoma (Hep2), breast adenocarcinoma (MCF7), and non-tumor human fibroblast cells (MRC5) by staining with Hoechst 33342/propidium iodide fluorescent dyes. The cytotoxic effect was evaluated by three parameters: live, dead, and apoptotic cell procentage. Cisplatin was tested under the same conditions and applied as the reference drug. After 48 h incubation of the mentioned cells with the tested compounds, the LC_{50} values (i.e., the compound concentration at which the number of live cells decreases by 50% compared to the control) are listed in Table 4.

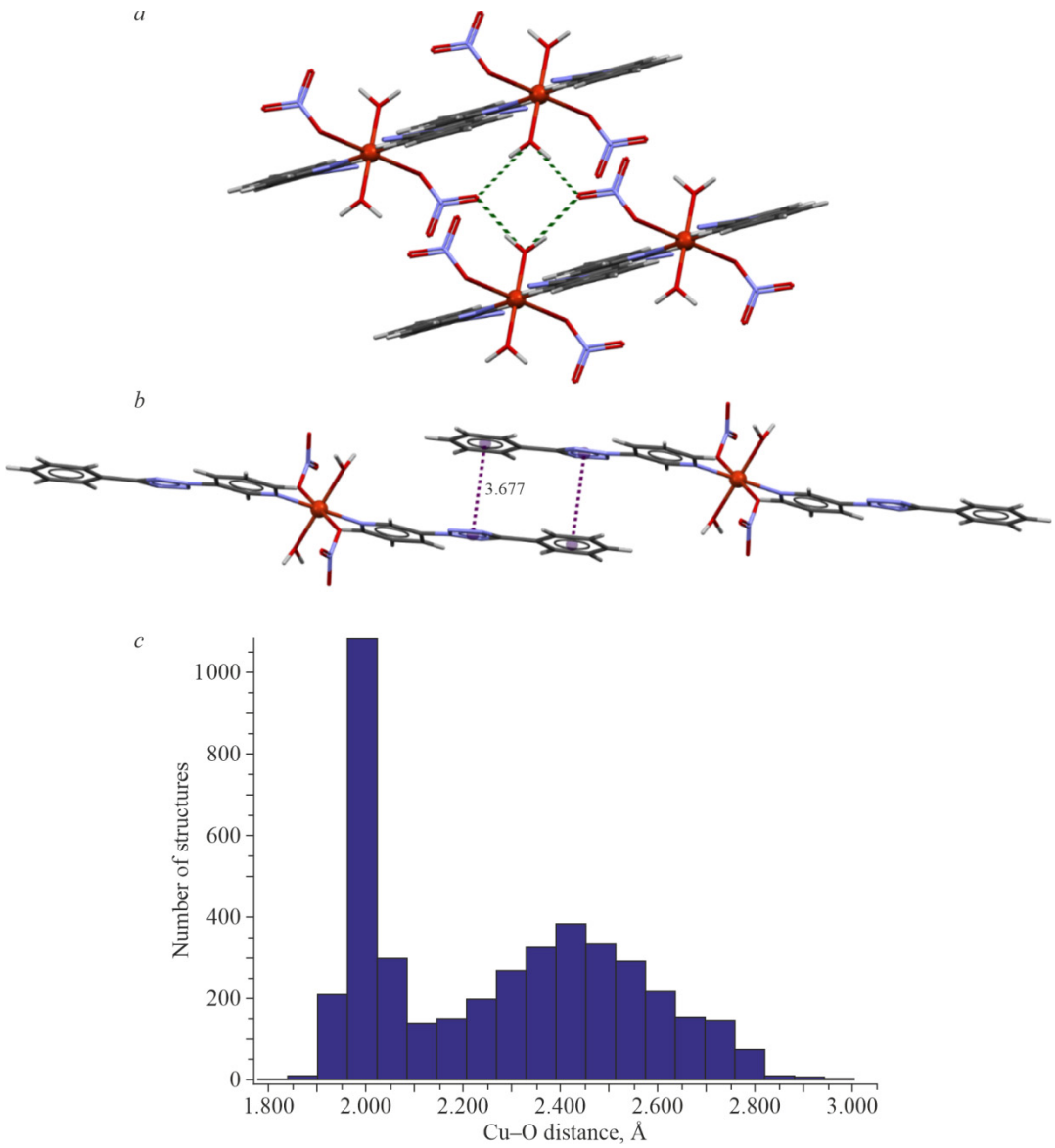

Fig. 11. Hydrogen bonds (*a*) and intermolecular π–π interactions (*b*) in the structure of complex **2a**. Histogram of Cu–O(NO_2) distances in the structures of copper nitrate compounds found in CCDC (*c*).

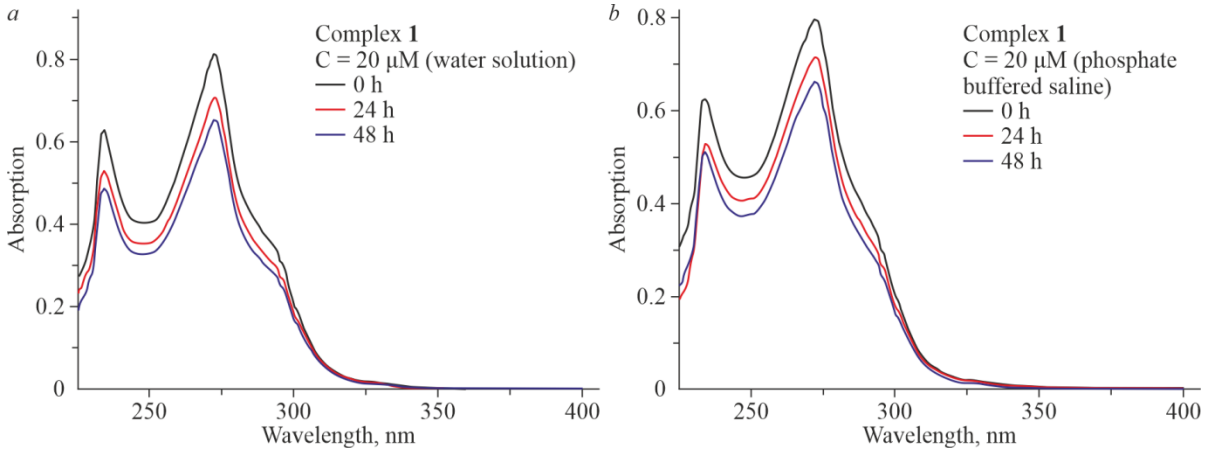

Fig. 12. Electronic absorption spectrum of complex **1**: aqueous solution (*a*) and phosphate buffer (*b*) at $t = 0$ h, 24 h, 48 h.

TABLE 3. Molar Extinction Coefficient for Complex **1** in the Aqueous Solution (H_2O) and Phosphate-Salt Buffer (PbS)

Solution	ε_1, $M^{-1}.cm^{-1}$	λ_1, nm	ε_2, $M^{-1}.cm^{-1}$	λ_2, nm
H_2O	$3.1 \cdot 10^4$	234	$4.1 \cdot 10^4$	272
PbS	$3.1 \cdot 10^4$	234	$4.0 \cdot 10^4$	272

TABLE 4. LC_{50} Values for the Ligands, Complex **1**, and Cisplatin

Compound	LC_{50}, μM			Reference
	Hep2	MCF7	MRC5	
Complex **1**	4.1±0.4	4.9±0.1	3.06±0.02	This work
L	–	>50	>50	
Phen	>50	42.5±3.7	>50	[35]
$Cu(NO_3)_2$	–	58.7±7.6	>50	[43]
Cisplatin	9.2±0.5	33.7±1.8	>50	[35, 44]

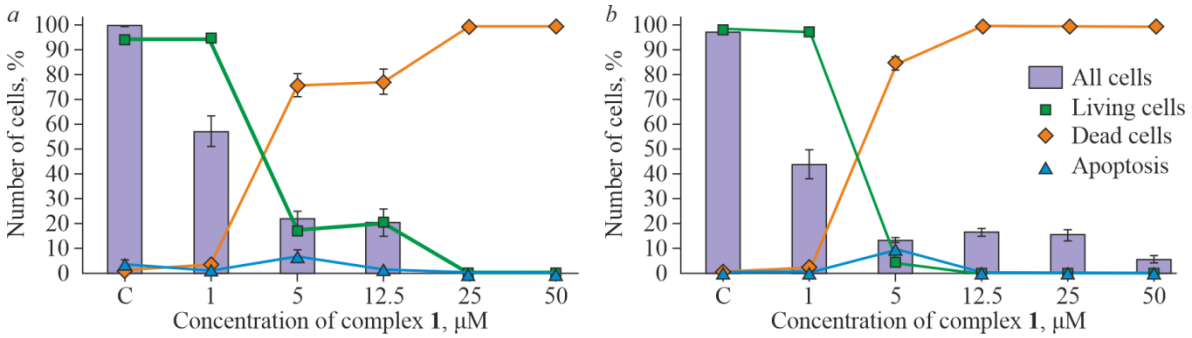

Fig. 13. Cytotoxic effect of complex **1** against the Hep2 (*a*) and MRC5 (*b*) cell lines.

In the studied concentration range (1-50 μM) for 48 h, ligands and copper(II) salt used do not produce the cytotoxic effect against Hep2 and MCF7 cell lines, except 1,10-phenanthroline that is cytotoxic against larynx carcinoma cells (LC_{50} = 42.5±3.7 μM). In the concentration range selected, complex **1** has a pronounced dose-dependent cytotoxic effect on both tumor cell lines (Fig. 13). Its activity surpasses that of cisplatin (reference drug) by an order of magnitude (Table 4). By comparing LC_{50} of initial reagents and complex **1** it can be seen that the cytotoxic properties are enhanced during complexation.

The cytotoxic activity against non-tumor human lung fibroblast cells (MRC5) was additionally studied. As in the case of Hep2 and MCF7, cytotoxicity of initial reagents was not detected in the range studied (1-50 μM), whereas compound **1** exhibited more active cytotoxic properties (LC_{50} = 3.06±0.02 μM, Fig. 13). The selectivity index representing the ratio of LC_{50} (MRC5) to LC_{50} (Hep2 or MCF7) is less than unity for compound **1**, which indicates the absence of the selective action of the complex obtained against tumor cell lines.

CONCLUSIONS

Five copper(II) coordination compounds based on 3-(5-phenyl-2H-tetrazol-2-yl)pyridine with additional ligands are synthesized and structurally characterized: 1,10-phenanthroline (**1**) or 2,2′-bipyridine and its derivatives (**2**, **3**). All complexes are mononuclear compounds in which 3-(5-phenyl-2*H*-tetrazol-2-yl)pyridine is coordinated by the nitrogen atom of the pyridine ring. The coordination polyhedron of **1** can be described by either vacant octahedron or square pyramid, but the

elongated Cu–O bond results in the 5 + 1 environment. We failed to unambiguously determine the coordination polyhedron for compound **2**, which is indicated by the τ_5 parameter value. Complex **3** has two non-equivalent copper atoms: Cu1 (5 + 2 coordination environment) and Cu2 (coordination polyhedron is vacant octahedron or square pyramid with the 5 + 1 environment). Coordination polyhedra of complexes **2a** and **3a** are the octahedron and the square with the 4 + 2 coordination environment respectively. Furthermore, intermolecular π–π interactions are present in all structures of the complexes.

The behavior of compound **1** was studied in both aqueous and phosphate-salt solutions for 48 h. It is shown that the form appeared after dissolution of the complex is unstable during the time interval studied. Moreover, the cytotoxic activity of this compound was investigated on non-tumor (MRC5) and tumor (Hep2, MCF7) cell lines. Complex **1** has the pronounced cytotoxic effect but it is non-selective against the tumor cell lines studied because the selectivity index is less than unity for both tumor cell lines.

ACKNOWLEDGMENTS

The authors would like to thank A. P. Zubareva for performing the elemental analysis, A. A. Shapovalova for measuring IR spectra, T. S. Sukhikh for providing the data obtained at the Multi-Access XRD Center of the Nikolaev Institute of Inorganic Chemistry, Siberian Branch, Russian Academy of Sciences, and M. O. Matveeva for performing the powder XRD analysis.

FUNDING

The work was supported by the Ministry of Science and Higher Education of the Russian Federation (project No. 121031700321-3). Experiments on the analysis of cytotoxicity were performed using the facilities of the Multi-Access Proteomic Analysis Center at the Federal Research Center of Fundamental and Translational Medicine and supported by the Ministry of Science and Higher Education of the Russian Federation (project No. 122032200236-1).

CONFLICT OF INTERESTS

The authors of this work declare that they have no conflicts of interest.

REFERENCES

1. J. Massin, L. Ducasse, T. Toupance, and C. Olivier. Tetrazole as a new anchoring group for the functionalization of TiO_2 nanoparticles: A joint experimental and theoretical study. *J. Phys. Chem. C*, **2014**, *118*(20), 10677-10685. https://doi.org/10.1021/jp502488g
2. L. Stolzer, A. Vigovskaya, C. Barner-Kowollik, and L. Fruk. A self-reporting tetrazole-based linker for the biofunctionalization of gold nanorods. *Chem. - Eur. J.*, **2015**, *21*(41), 14309-14313. https://doi.org/10.1002/chem.201502070
3. M. N. Nichick, S. V. Voitekhovich, V. Lesnyak, V. E. Matulis, R. A. Zheldakova, A .I. Lesnikovich, and O. A. Ivashkevich. 1-Substituted tetrazole-5-thiol-capped noble metal nanoparticles. *J. Phys. Chem. C*, **2011**, *115*(34), 16928-16933. https://doi.org/10.1021/jp205649y
4. E. Ocansey, J. Darkwa, and B. C. E. Makhubela. Chiral-at-metal: Iridium(III) tetrazole complexes with proton-responsive P–OH groups for CO_2 hydrogenation. *Front. Chem.*, **2020**, *8*, 591353. https://doi.org/10.3389/fchem.2020.591353
5. E. Ocansey, J. Darkwa, and B. C. E. Makhubela. CO_2 conversion to formates catalyzed by iridium(III) catalysts precursors with proton responsive OH and NH electron-rich tetrazole ligands. *Mol. Catal.*, **2022**, *517*, 111979. https://doi.org/10.1016/j.mcat.2021.111979

6. M. Nasrollahzadeh, Z. Nezafat, N. S. S. Bidgoli, and N. Shafiei. Use of tetrazoles in catalysis and energetic applications: Recent developments. *Mol. Catal.*, **2021**, *513*, 111788. https://doi.org/10.1016/j.mcat.2021.111788
7. V. A. Ostrovskii, E. N. Chernova, Z. A. Zhakovskaya, Y. N. Pavlyukova, M. A. Ilyushin, and R. E. Trifonov. Decomposition products of tetrazoles as starting reagents of secondary chemical and biochemical reactions. *Russ. Chem. Rev.*, **2024**, *93*(8), RCR5118. https://doi.org/10.59761/rcr5118
8. A. I. Lesnikovich, S. V. Levchik, A. I. Balabanovich, O. A. Ivashkevich, and P. N. Gaponik. The thermal decomposition of tetrazoles. *Thermochim. Acta*, **1992**, *200*, 427-441. https://doi.org/10.1016/0040-6031(92)85135-i
9. F. Gao, J. Xiao, and G. Huang. Current scenario of tetrazole hybrids for antibacterial activity. *Eur. J. Med. Chem.*, **2019**, *184*, 111744. https://doi.org/10.1016/j.ejmech.2019.111744
10. J. Dudley, L. Feinn, H. DeFrancesco, E. Lindsay, A. Coca, and E. L. Roberts. Antibacterial assessment of heteroaryl, vinyl, benzyl, and alkyl tetrazole compounds. *Med. Chem.*, **2018**, *14*(6), 550-555. https://doi.org/10.2174/1573406413666171120162420
11. Z. H. Chohan, M. Arif, Z. Shafiq, M. Yaqub, and C. T. Supuran. In vitro antibacterial, antifungal & cytotoxic activity of some isonicotinoylhydrazide Schiff's bases and their cobalt(II), copper(II), nickel(II) and zinc(II) complexes. *J. Enzyme Inhib. Med. Chem.*, **2006**, *21*(1), 95-103. https://doi.org/10.1080/14756360500456806
12. M. Devi, S. Jaiswal, N. Yaduvanshi, N. Kaur, D. Kishore, J. Dwivedi, and S. Sharma. Design, synthesis, antibacterial evaluation and docking studies of triazole and tetrazole linked 1,4-benzodiazepine nucleus *via* click approach. *ChemistrySelect*, **2023**, *8*(6), e202204710. https://doi.org/10.1002/slct.202204710
13. E. A. Popova, R. E. Trifonov, and V. A. Ostrovskii. Tetrazoles for biomedicine. *Russ. Chem. Rev.*, **2019**, *88*(6), 644-676. https://doi.org/10.1070/rcr4864
14. A. Poliakov, A. Johansson, E. Åkerblom, K. Oscarsson, B. Samuelsson, A. Hallberg, and U. H. Danielson. Structure–activity relationships for the selectivity of hepatitis C virus NS3 protease inhibitors. *Biochim. Biophys. Acta, Gen. Subj.*, **2004**, *1672*(1), 51-59. https://doi.org/10.1016/j.bbagen.2004.02.008
15. A. Johansson, A. Poliakov, E. Åkerblom, K. Wiklund, G. Lindeberg, S. Winiwarter, U. H. Danielson, B. Samuelsson, and A. Hallberg. Acyl sulfonamides as potent protease inhibitors of the hepatitis C virus full-Length NS3 (protease-helicase/NTPase): A comparative study of different C-terminals. *Bioorg. Med. Chem.*, **2003**, *11*(12), 2551-2568. https://doi.org/10.1016/s0968-0896(03)00179-2
16. A. V. Khramchikhin, M. A. Skryl′nikova, M. A. Gureev, V. V. Zarubaev, I. L. Esaulkova, P. A. Ilyina, O. A. Mammeri, D. V. Spiridonova, Y. B. Porozov, and V. A. Ostrovskii. Novel 1,2,4-triazole- and tetrazole-containing 4h-thiopyrano[2,3-b]quinolines: Synthesis based on the thio-michael/aza-morita–baylis–hillman tandem reacion and investigation of antiviral activity. *Molecules*, **2023**, *28*(21), 7427. https://doi.org/10.3390/molecules28217427
17. O. V. Mikolaichuk, V. V. Zarubaev, A. A. Muryleva, Y. L. Esaulkova, D. V. Spasibenko, A. A. Batyrenko, I. V. Kornyakov, and R. E. Trifonov. Synthesis, structure, and antiviral properties of novel 2-adamantyl-5-aryl-2H-tetrazoles. *Chem. Heterocycl. Compd.*, **2021**, *57*, 442-447. https://doi.org/10.1007/s10593-021-02931-5
18. M. A. Kale, R. B. Nawale, M. R. Peharkar, and S. V. Kuberkar. Synthesis and pharmacological evaluation of tetrazolobenzimidazoles as novel anti-inflammatory agents. *Anti-Inflammatory Anti-Allergy Agents Med. Chem.*, **2016**, *15*(2), 118-126. https://doi.org/10.2174/1871523015666160915153904
19. A. Hussain, M. F. AlAjmi, M. T. Rehman, S. Amir, F. M. Husain, A. Alsalme, M. A. Siddiqui, A. A. AlKhedhairy, and R. A. Khan. Copper(II) complexes as potential anticancer and nonsteroidal anti-inflammatory agents: In vitro and in vivo studies. *Sci. Rep.*, **2019**, *9*(1), 5237. https://doi.org/10.1038/s41598-019-41063-x
20. A. A. Bekhit, O. A. El-Sayed, E. Aboulmagd, and J. Y. Park. Tetrazolo[1,5-a]quinoline as a potential promising new scaffold for the synthesis of novel anti-inflammatory and antibacterial agents. *Eur. J. Med. Chem.*, **2004**, *39*(3), 249-255. https://doi.org/10.1016/j.ejmech.2003.12.005

21. M. B. Labib, A. M. Fayez, E.-S. EL-Nahass, M. Awadallah, and P. A. Halim. Novel tetrazole-based selective COX-2 inhibitors: Design, synthesis, anti-inflammatory activity, evaluation of PGE2, TNF-α, IL-6 and histopathological study. *Bioorg. Chem.*, **2020**, *104*, 104308. https://doi.org/10.1016/j.bioorg.2020.104308
22. S.-Q. Wang, Y.-F. Wang, and Z. Xu. Tetrazole hybrids and their antifungal activities. *Eur. J. Med. Chem.*, **2019**, *170*, 225-234. https://doi.org/10.1016/j.ejmech.2019.03.023
23. M. A. Malik, S. A. Al-Thabaiti, and M. A. Malik. Synthesis, structure optimization and antifungal screening of novel tetrazole ring bearing acyl-hydrazones. *Int. J. Mol. Sci.*, **2012**, *13*(9), 10880-10898. https://doi.org/10.3390/ijms130910880
24. A. G. S. Warrilow, C. M. Hull, J. E. Parker, E. P. Garvey, W. J. Hoekstra, W. R. Moore, R. J. Schotzinger, D. E. Kelly, and S. L. Kelly. The clinical candidate VT-1161 is a highly potent inhibitor of candida albicans CYP51 but fails to bind the human enzyme. *Antimicrob. Agents Chemother.*, **2014**, *58*(12), 7121-7127. https://doi.org/10.1128/aac.03707-14
25. R. S. Upadhayaya, S. Jain, N. Sinha, N. Kishore, R. Chandra, and S. K. Arora. Synthesis of novel substituted tetrazoles having antifungal activity. *Eur. J. Med. Chem.*, **2004**, *39*(7), 579-592. https://doi.org/10.1016/j.ejmech.2004.03.004
26. R. E. Trifonov and V. A. Ostrovskii. Tetrazoles and related heterocycles as promising synthetic antidiabetic agents. *Int. J. Mol. Sci.*, **2023**, *24*(24), 17190. https://doi.org/10.3390/ijms242417190
27. N. Dhiman, K. Kaur, and V. Jaitak. Tetrazoles as anticancer agents: A review on synthetic strategies, mechanism of action and SAR studies. *Bioorg. Med. Chem.*, **2020**, *28*(15), 115599. https://doi.org/10.1016/j.bmc.2020.115599
28. E. A. Popova, A. V. Protas, and R. E. Trifonov. Tetrazole derivatives as promising anticancer agents. *Anticancer. Agents Med. Chem.*, **2018**, *17*(14), 1856-1868. https://doi.org/10.2174/1871520617666170327143148
29. J. Zhang, S. Wang, Y. Ba, and Z. Xu. Tetrazole hybrids with potential anticancer activity. *Eur. J. Med. Chem.*, **2019**, *178*, 341-351. https://doi.org/10.1016/j.ejmech.2019.05.071
30. A. V. Subba Rao, K. Swapna, S. P. Shaik, V. Lakshma Nayak, T. Srinivasa Reddy, S. Sunkari, T. B. Shaik, C. Bagul, and A. Kamal. Synthesis and biological evaluation of *cis*-restricted triazole/tetrazole mimics of combretastatin-benzothiazole hybrids as tubulin polymerization inhibitors and apoptosis inducers. *Bioorg. Med. Chem.*, **2017**, *25*(3), 977-999. https://doi.org/10.1016/j.bmc.2016.12.010
31. J. A. Eremina, E. V. Lider, N. V. Kuratieva, D. G. Samsonenko, L. S. Klyushova, D. G. Sheven′, R. E. Trifonov, and V. A. Ostrovskii. Synthesis and crystal structures of cytotoxic mixed-ligand copper(II) complexes with alkyl tetrazole and polypyridine derivatives. *Inorg. Chim. Acta*, **2021**, *516*, 120169. https://doi.org/10.1016/j.ica.2020.120169
32. J. A. Eremina, K. S. Smirnova, L. S. Klyushova, A. S. Berezin, and E. V. Lider. Synthesis and cytotoxicity evaluation of copper(II) complexes with polypyridines and 5-benzyltetrazole. *J. Mol. Struct.*, **2021**, *1245*, 131024. https://doi.org/10.1016/j.molstruc.2021.131024
33. J. A. Eremina, E. A. Ermakova, K. S. Smirnova, L. S. Klyushova, A. S. Berezin, T. S. Sukhikh, A. A. Zubenko, L. N. Fetisov, K. N. Kononenko, and E. V. Lider. Cu(II), Co(II), Mn(II) complexes with 5-phenyltetrazole and polypyridyl ligands: Synthesis, characterization and evaluation of the cytotoxicity and antimicrobial activity. *Polyhedron*, **2021**, *206*, 115352. https://doi.org/10.1016/j.poly.2021.115352
34. Y. A. Golubeva, K. S. Smirnova, L. S. Klyushova, A. S. Berezin, and E. V. Lider. Cytotoxic copper(II) complexes based on 2,2′-bipyridine/1,10-phenanthroline and 5-(4-chlorophenyl)-1H-tetrazole: Synthesis and structures. *Russ. J. Coord. Chem.*, **2023**, *49*(9), 528-541. https://doi.org/10.1134/s1070328423600110
35. E. A. Ermakova, Y. A. Golubeva, K. S. Smirnova, L. S. Klyushova, A. S. Berezin, L. N. Fetisov, A. E. Svyatogorova, N. O. Andros, A. A. Zubenko, and E. V. Lider. Cytotoxic mixed-ligand copper(II) complexes with 1*H*-tetrazole-5-acetic acid and oligopyridine derivatives. *New J. Chem.*, **2023**, *47*(19), 9472-9482. https://doi.org/10.1039/d3nj00568b
36. I. S. Ershov, K. A. Esikov, O. M. Nesterova, M. A. Skryl′nikova, A. V. Khramchikhin, N. T. Shmaneva, I. S. Chernov, E. N. Chernova, A. M. Puzyk, E. V. Sivtsov, Y. N. Pavlyukova, R. E. Trifonov, and V. A. Ostrovskii. 3-(5-Phenyl-2H-tetrazol-2-yl)pyridine. *Molbank*, **2023**, *2023*(1), M1598. https://doi.org/10.3390/m1598

37. APEX2 (Version 2.0), SAINT (Version 8.18c) and SADABS (Version 2.11). Madison, WI, USA: Bruker AXS, **2000-2012**.
38. G. M. Sheldrick. SHELXT - Integrated space-group and crystal-structure determination. *Acta Crystallogr*., *Sect. A: Found. Adv.*, **2015**, *71*(1), 3-8. https://doi.org/10.1107/s2053273314026370
39. G. M. Sheldrick. Crystal structure refinement with SHELXL. *Acta Crystallogr*., *Sect. C: Struct. Chem.*, **2015**, *71*(1), 3-8. https://doi.org/10.1107/s2053229614024218
40. O. V. Dolomanov, L. J. Bourhis, R. J. Gildea, J. A. K. Howard, and H. Puschmann. OLEX2: a complete structure solution, refinement and analysis program. *J. Appl. Crystallogr.*, **2009**, *42*(2), 339-341. https://doi.org/10.1107/s0021889808042726
41. A. W. Addison, T. N. Rao, J. Reedijk, J. van Rijn, and G. C. Verschoor. Synthesis, structure, and spectroscopic properties of copper(II) compounds containing nitrogen–sulphur donor ligands; the crystal and molecular structure of aqua[1,7-bis(N-methylbenzimidazol-2′-yl)-2,6-dithiaheptane]copper(II) perchlorate. *J. Chem. Soc*., *Dalton Trans.*, **1984**, (7), 1349-1356. https://doi.org/10.1039/dt9840001349
42. L. Yang, D. R. Powell, and R. P. Houser. Structural variation in copper(I) complexes with pyridylmethylamide ligands: structural analysis with a new four-coordinate geometry index, τ_4. *Dalton Trans.*, **2007**, (9), 955-964. https://doi.org/10.1039/b617136b
43. Y. P. Tupolova, L. D. Popov, V. G. Vlasenko, K. B. Gishko, A. A. Kapustina, A. G. Berejnaya, Y. A. Golubeva, L. S. Klyushova, E. V. Lider, V. A. Lazarenko, S. S. Bachurin, and I. N. Shcherbakov. Crystal structure and cytotoxic activity of Cu(II) complexes with bis-benzoxazolylhydrazone of 2,6-diacetylpyridine. *New J. Chem.*, **2023**, *47*(31), 14972-14985. https://doi.org/10.1039/d3nj02445h
44. E. A. Ermakova, Y. A. Golubeva, K. S. Smirnova, L. S. Klyushova, and E. V. Lider. Structure and cytotoxic activity of the manganese(II) complex with 5-methyltetrazole and 4,7-dimethyl-1,10-phenanthroline. *J. Struct. Chem.*, **2023**, *64*(4), 540-549. https://doi.org/10.1134/s0022476623040029